Demonstration of a modular, scalable, laser communication terminal for manned spaceflight missions

Steven R. Gillmer, Corrie V. Smeaton, Jamie W. Burnside, James Torres, William Hubbard, Casey Bennett, Catherine DeVoe, John A. Wellman, Justin J. Rey, Michael J. Zervas, Farzana I. Khatri, Tina Shih, Owen Guldner, Mark Padula, Bryan S. Robinson

Massachusetts Institute of Technology Lincoln Laboratory, Lexington, MA 02421, USA

ABSTRACT

Free-space laser communication systems are increasingly implemented on state of the art satellites for their high-speed connectivity. This work outlines a demonstration of the Modular, Agile, Scalable Optical Terminal (MAScOT) we have developed to support Low-Earth Orbit (LEO) to deep-space communication links. In LEO, the MAScOT will be implemented on the International Space Station to support the Integrated Laser Communications Relay Demonstration (LCRD) LEO User Modem and Amplifier Terminal (ILLUMA-T) program. ILLUMA-Ts overarching objective is to demonstrate high bandwidth data transfer between LEO and a ground station via a geosynchronous (GEO) relay satellite. Outside of GEO, MAScOT will also be implemented on the Artemis-II mission to demonstrate high data rate optical communications to and from the moon as part of the Orion EM-2 Optical Communications (O2O) program. Both missions leverage the same modular architecture despite varying structural, thermal, and optical requirements. To achieve sufficient performance, the optical terminal relies on a nested tracking loop to realize sub-arcsecond pointing across $\pm 120^\circ$ elevation and $\pm 175^\circ$ azimuth field of regard.

Keywords: Laser Communication, Gimbal, Nested Control Tracking, Space Mechanisms, Fast Steering Mirror

1. INTRODUCTION

The emergence of more capable instruments onboard spacecraft is driving an increasing need for high-bandwidth communications. Furthermore, as deep-space missions are becoming more prevalent, high signal-to-noise ratio (SNR) links are essential for reliable data transfer across vast distances. For these reasons, laser communication offers unique advantages compared to radio frequency (RF) communication. In addition to increased SNR, laser communication links require reduced size, weight, and power for adequate performance.

The current work builds on the success of past laser communication efforts at MIT Lincoln Laboratory, including the Lunar Laser Communications Demonstration (LLCD).[1,2] The LLCD lasercom link successfully demonstrated 20 Mbps uplink, 622 Mbps downlink data transfer to and from the moon. The LLCD terminal exceeded mission requirements, and the initial design is now transforming to serve on a variety of future satellites ranging from low-earth orbit (LEO) to geosynchronous orbit (GEO) and beyond in to deep-space. In particular there is a desire to increase the $\pm 20^\circ$ field of regard (FOR) of the LLCD optical module.

In this proceedings we describe the ongoing design and lab-performance of a next generation laser communication terminal - the the Modular, Agile, Scalable Optical Terminal (MAScOT).[3,4] In LEO, the MAScOT will be implemented on the International Space Station to support the Integrated Laser Communications Relay Demonstration (LCRD) LEO User Modem and Amplifier Terminal (ILLUMA-T) program. ILLUMA-Ts overarching objective is to demonstrate high bandwidth data transfer between LEO and a ground station via a GEO relay satellite. Outside of GEO, MAScOT will also be implemented on the Artemis-II mission to demonstrate high data rate optical communications to and from the moon as part of the Orion EM-2 Optical Communications (O2O) program. Both ILLUMA-T and O2O require wide-FOR performance to meet mission goals. As a result, the MAScOT was designed to support sub-arcsecond beam pointing across $\pm 120^\circ$ elevation and $\pm 175^\circ$ azimuth FOR.

Further author information: (Send correspondence to S.R.G)
S.R.G: E-mail: steven.gillmer@ll.mit.edu, Telephone: +1 (781) 981-1721

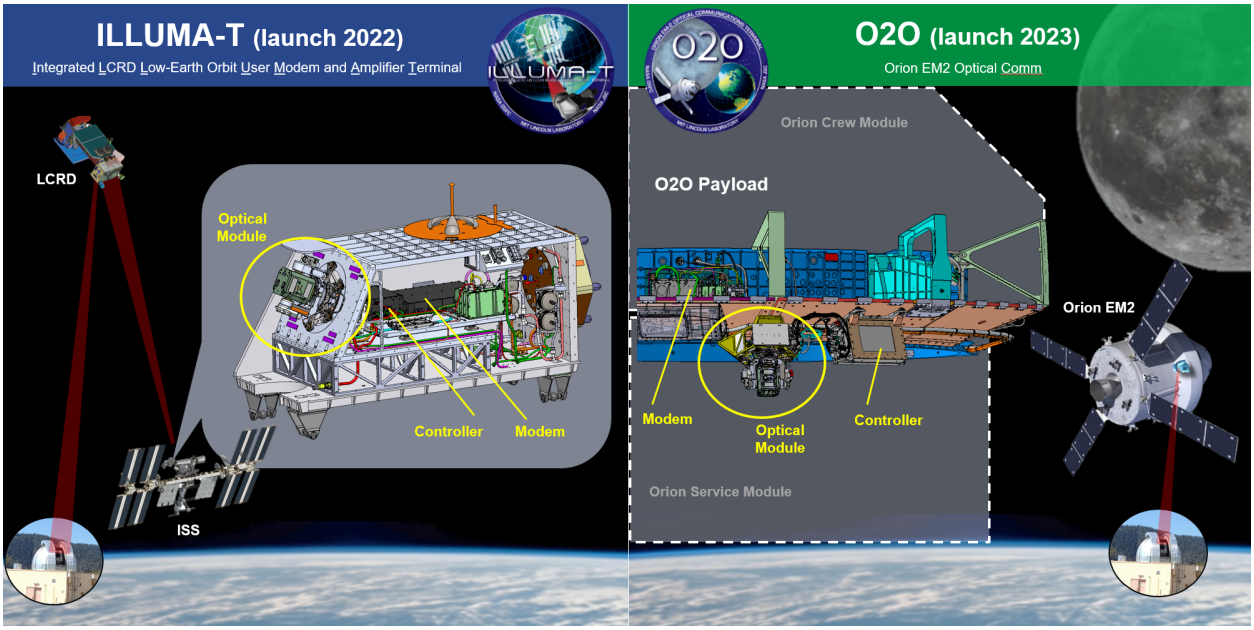

Figure 1. Overview of the ILLUMA-T and O2O missions. Both missions leverage the same laser communication terminal as described in this proceedings.

The following discussion with outline the optomechanical design of the MAScOT. Emphasis will be placed on the design of the nested tracking control system which enables precision pointing across such a large range of the system's gimbal. Preliminary wavefront and tracking performance of the terminal will be presented.

2. DESIGN OF THE OPTICAL MODULE

The MAScOT optical module is designed as a modular system. The major subcomponents are outlined in Figure 2. MIT Lincoln Laboratory (MIT LL) designs and integrates the overall system; however, the design, build, and integration of various subcomponents is performed by industry partners as outlined in Figure 2. The core of the terminal is the Latch and Gimbal Assembly (LGA) which is composed of an 2-axis gimbal with a ± 175 and ± 120 range of motion in Azimuth and Elevation, respectively. The LGA also has an integrated latch to restrain the optical module during launch. To align the Optical Module, the Backend Optical Assembly (BOA) is mounted to the LGA first and aligned to the rotational axis of the azimuth axis using the transmit beam. After aligning the optical BOA axis to the mechanical azimuth axis of the LGA, the Relay assembly as part of the Telescope and Relay Assembly (TRA) mounts to the LGA to route the coudé path through the outrigger arm of the elevation yoke. The Fold Mirror Assembly (which is part of the LGA) folds the coudé path in to the Telescope. The entire optical assembly sits on vibration isolators to minimize loading during launch in addition to minimizing jitter on-orbit. Finally all of the optical module is controlled through a Thermal Control System (TCS) which is designed and analyzed by MIT LL to keep the components within operational temperature limits and keep the optical module performance within mission requirements.

2.1 Optical Design

The transmit and receive optical paths of the MAScOT are required to be co-boresighted relative to eachother within 0.83 arcsec (4 µrad). Furthermore, the far-field beam pointing must be accurate to within the same tolerance. To achieve this level of precision, two fundamental optical design implementations exist: first, three separate steering mirrors are implemented in the BOA to maintain pointing; and second, a nominal 43.25X magnification (1.73X through the RA and an additional 25X through the TA) scales pointing changes in the BOA out of the optical module. The magnification factor magnifies decenter runout from small beam space but has the coupled advantage of de-magnifying angular pointing. That is, a 35 arcsecond ($\sim$170 µrad) pointing

change from a steering mirror in the BOA translates to a 0.8 arcsec (3.9 µrad) pointing change coming out of the TA. This magnification factor enables high precision angular beam pointing without exceedingly complex beam steering mechanisms.

A schematic of the MAScOT and BOA is shown in Figure 3. Within the BOA, optical signals are steered with the Fast-Steering Mirror (FSM), Look-Behind Mirror (LBM), and Hand-Over Mirror (HOM). Beam paths are isolated using Narrorow Bandpass Filters (NBF) and wavelength-selective beamsplitters (BS). The control system and its implementation in this architecture will be described subsequently; however, from a high level the optical beam steering approach is as follows: The FSM controls high-bandwidth disturbances as measured

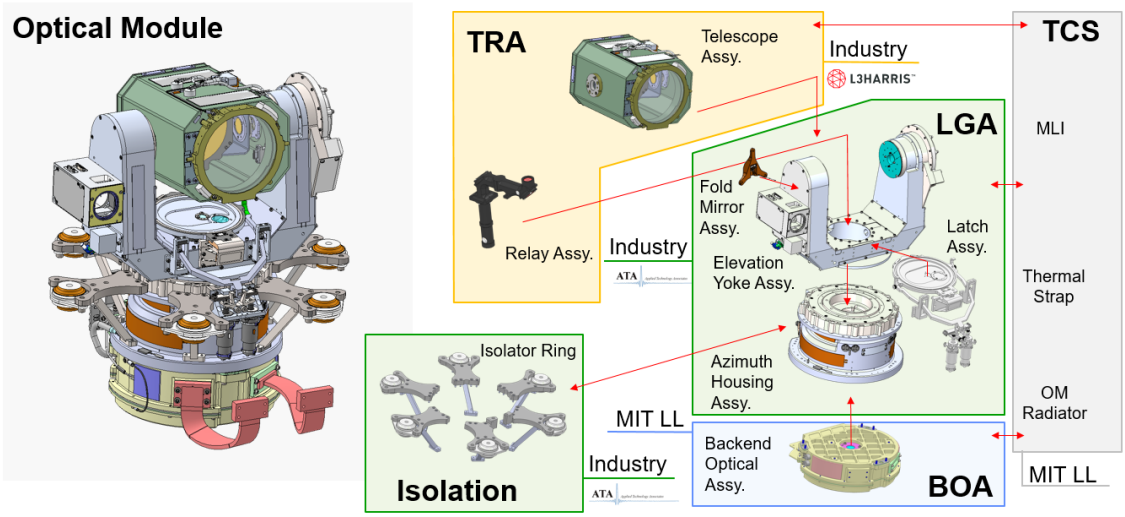

Figure 2. Subassemblies of the MAScOT. These subcomponents are designed to be modular in nature to meet various mission goals (TRA - Telescope and Relay Assembly, LGA - Latch and Gimbal Assembly, TCS - Thermal Control System, BOA - Backend Optical Assembly, MLI - Multi-layer Insulation).

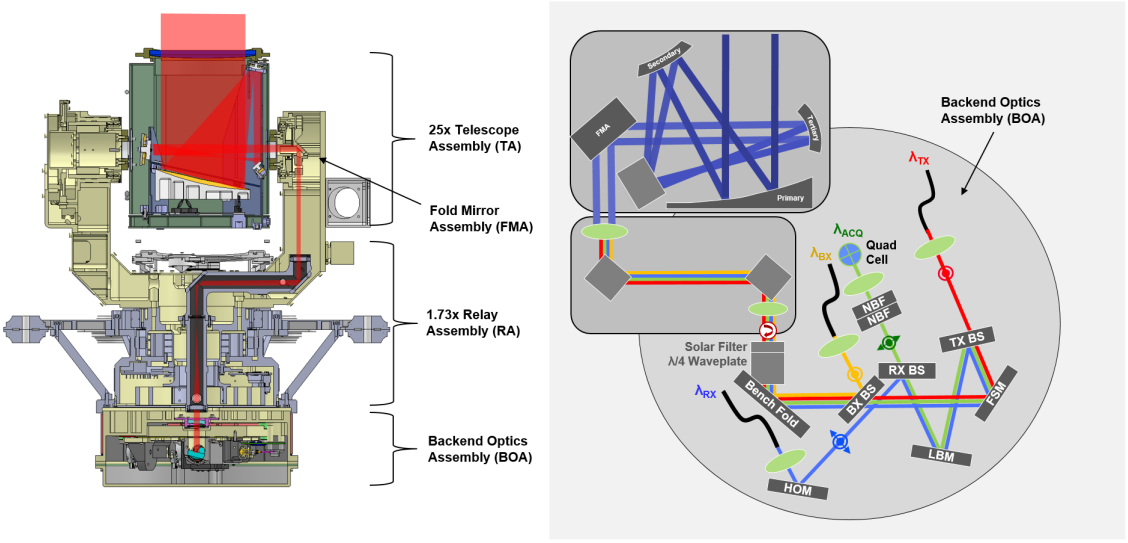

Figure 3. Schematic of the optical module. The system has a nominal full magnification of 43.25X which is divided in to 25X through the TA and 1.73X through the RA (FSM - Fast-Steering Mirror, LBM - Look-Behind Mirror, HOM - Hand-Over Mirror, NBF - Narrow Bandpass Filter, TX - Transmit Path, ACQ - Acquisition Path, BX - Beacon Path, RX - Receive path, BS - Beamsplitter).

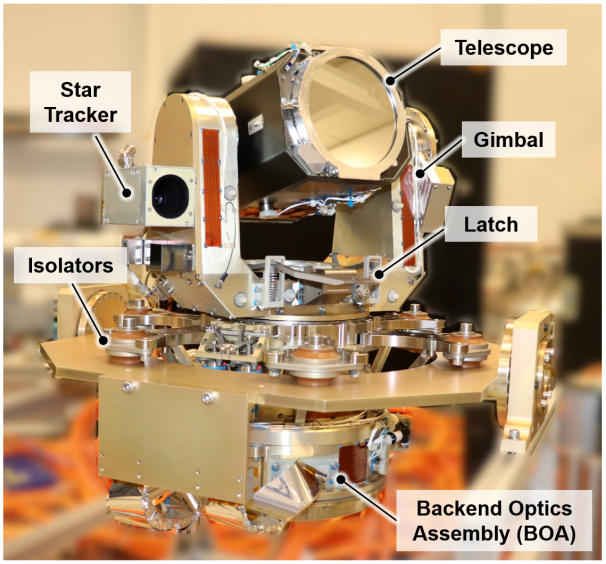

Figure 4. The as-built O2O optical module.

by the Quad Detector (up to nominally ~200 Hz), the LBM steers the Acquisition beam to the center of the Quad Detector and offsets pointing biases on the FSM, and the HOM operates with a hill-climbing algorithm to optimize coupling in to the RX fiber.

For representative performance of the TX channel of the O2O OM, its performance at ambient conditions is shown in Figure 5. The wavefront changes as a function of the Azimuth and Elevation pointing of the gimbal, and as such, the wavefront error is listed as a function of gimbal pointing. For the RX channel, although not shown, a similar trend is observed which nominally agrees with budgeted values and does not show a bias in worse performance torwards a particular region of gimbal pointing.

2.2 Point, Acquisition, and Track

The optical module has been equipped with the capabilities to perform four fundamental autonomous tasks in order to establish a laser communication link: (1) Given its GPS coordinates and star tracker orientation, perform a general search in the area where a link will be established, (2) After receiving power from a beacon or acquisition

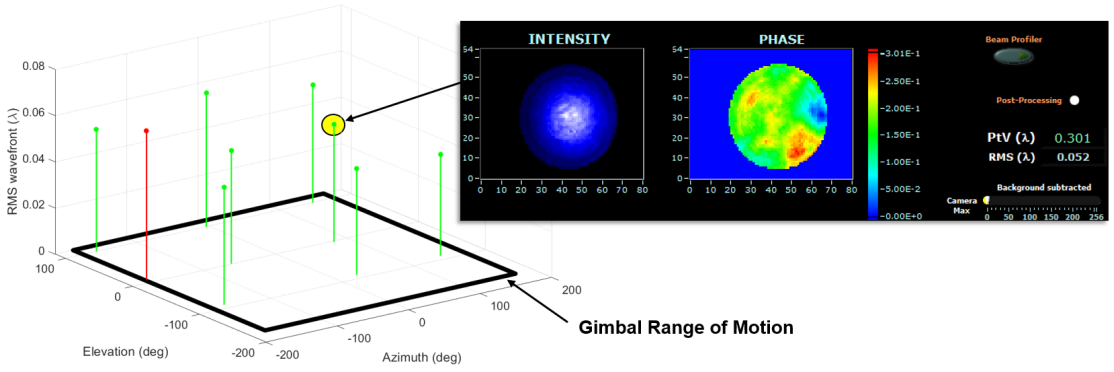

Figure 5. As-built ambient wavefront error of the O2O optical module. Values shown in green meet wavefront allocations for ambient requirements. The one value in red slightly exceeds specification but positive margin in other aspects of the optical module redeem sufficient performance.

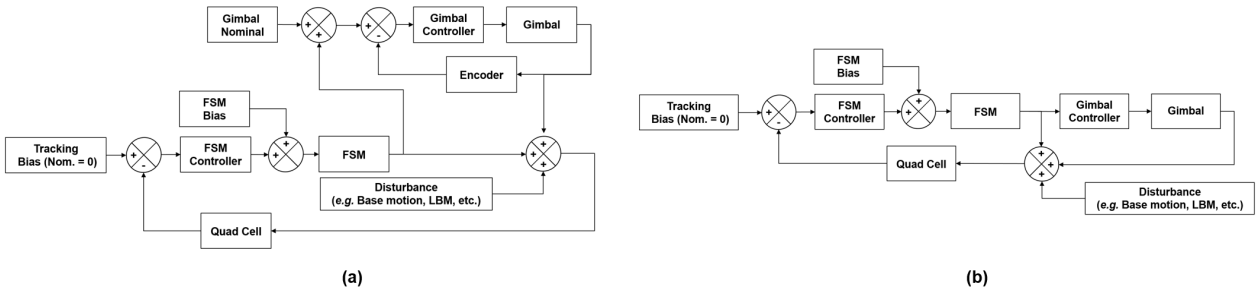

Figure 6. The point acquisition and track algorithm detects an initial signal on the quad, transitions to (a) cascaded tracking and eventually as it pulls in to better performance, transitions to (b) nested tracking.

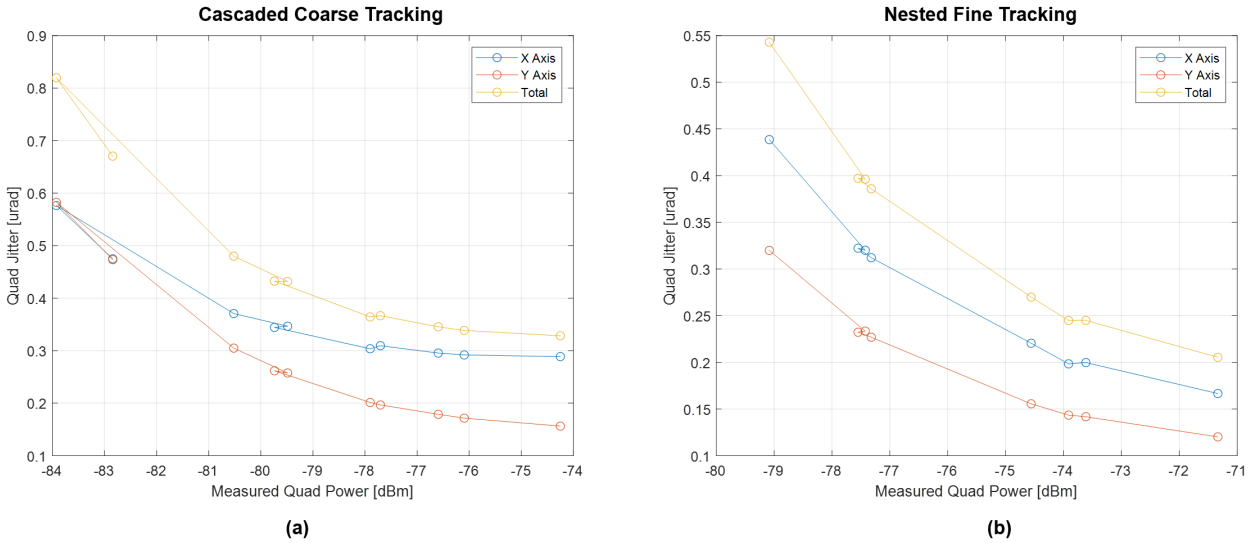

Figure 7. Performance of the optical module as measured by a calibrated high-speed camera under (a) cascaded tracking and eventually as it pulls in to better performance, transitions to (b) nested tracking. Performance is plotted as function of input Acquisition power to the optical module.

light source, engage in a pull-in spiral maneuver that maximizes light on the quadrant detector using the gimbal motion, (3) after acquiring acquisition light, engage in coarse tracking using a cascaded control architecture, and finally (4) enter fine track using a nested tracking loop and begin a communication link. The initial search using the star tracker relies on a careful calibration of the gimbal spin axes relative to the star tracker boresight. This calibration requires the knowledge of the gimbal axes relative to the star tracker within <62 arcsec (<300 µrad) radial error. As such, this is achievable assuming the implementation of ABEC 6 or ABEC 7 precision bearings with wobble on the order of <21 arcsec (<100 µrad).[5,6] For our results, the orientation was calibrated relative to precision alignment cubes mounted to the sides of the Azimuth and Elevation optical module. As the optical module rotates, the alignment cubes are tracked with theodolites and oriented to a global reference frame.

Mission requirements necessitate pointing performance under operational jitter conditions of <0.83 arcsec (<4 µrad). As the above process outlined, this is achieved through a transition from coarse tracking in a cascaded architecture to a fine track in a nested loop. Two diagrams outlining the control loops are shown in Figure 6 and the performance of both loops in a lab environment is shown in Figure 7. As can be seen in both loops, as the FSM begins to add a DC bias towards one end of its range of motion under tracking, the gimbal counteracts and offsets the FSM bias. For both loops, benchtop performance has demonstrated 190 Hz bandwidth of the cascaded control loop and 350 Hz bandwidth of the nested loop (bandwidth defined as 0 dB

crossover in the amplitude response of a Bode plot). More research is underway to examine performance under predicted operational jitter conditions, which will be discussed in a future publication.

3. CONCLUSIONS

The MAScOT system has been designed and built for implementation on a wide variety of mission environments at varying altitudes. Key enablers to its success as outlined in this work are precision beam pointing achieved through a magnified optical path and a combination of cascaded and nested control. Future testing will continue to evaluate the performance of the optical module against the ILLUMA-T and O2O mission goals.

ACKNOWLEDGMENTS

There are hundreds of team players who are working together to make these laser communication missions a success across multiple organizations. We thank our partners at MIT Lincoln Laboratory, NASA GSFC, NASA Johnson, JPL, Lockheed Martin, Marshall Space Flight Center, and Kennedy Space Center for all of the contributions to this work.

DISTRIBUTION STATEMENT A. Approved for public release. Distribution is unlimited.

This material is based upon work supported by the National Aeronautics and Space Administration under Air Force Contract No. FA8702-15-D-0001. Any opinions, findings, conclusions or recommendations expressed in this material are those of the author(s) and do not necessarily reflect the views of the National Aeronautics and Space Administration .

REFERENCES

[1] Boroson, D. M., Robinson, B. S., Murphy, D. V., Burianek, D. A., Khatri, F., Kovalik, J. M., Sodnik, Z., and Cornwell, D. M., "Overview and results of the lunar laser communication demonstration," in [*Free-Space Laser Communication and Atmospheric Propagation XXVI*], *Proc. SPIE* **8971** (2014).

[2] Nevin, K. E., Doyle, K. B., and Pullsbury, A. D., "Optomechanical design and analysis for the LLCD space terminal telescope," in [*Optical Modeling and Performance Predictions V*], *Proc. SPIE* **8127** (2011).

[3] Shih, T., DeVoe, C., Guldner, O., Hubbard, W., Khatri, F. I., Constantine, S., Burnside, J. W., Torres, J., and Robinson, B. S., "A modular, agile, scalable optical terminal architecture for space communications," in [*International Conference on Space Optical Systems and Applications (ICSOS)*], *Proc. IEEE* (2017).

[4] Robinson, B. S., Shih, T., Khatri, F. I., Boroson, D. M., Burnside, J. W., Guldner, O., Constantine, S., Torres, J., Yarnall, T. M., DeVoe, C. E., Hubbard, W., Geisler, D. J., Stevens, M. L., Mikulina, O., Spellmeyer, N. W., Wang, J. P., Butler, R., Hogan, M., King, T., and Seas, A., "Laser communications for human space exploration in cislunar space: ILLUMA-T and O2O," in [*Free-Space Laser Communication and Atmospheric Propagation XXX*], *Proc. SPIE* **10524** (2018).

[5] Gillmer, S., McMenamin, C., Powers, B., Racamato, J., DiLiberto, M., Cunningham, A., Fuhrman, L., Crompton, D., Michael, S., Clark, K., and Blackwell, W., "Precision scanning onboard the NASA TROPICS mission," *Proc. ASPE* (2018).

[6] Burnside, J. W., Conrad, S. D., Pillsbury, A. D., and DeVoe, C. E., "Design of an inertially stabilized telescope for the LLCD," in [*Free-Space Laser Communication and Atmospheric Propagation XXIII*], *Proc. SPIE* **7923** (2011).